Novel Contact Sensor Concept and Prototype based on 2-DOF Vibration Absorber System

Hussein F.M. Ali
Mechatronics and Robotics Engineering Dept.,
Egypt-Japan University of Science and Technology
Alexandria, Egypt
e-mail: hussein.ali@ejust.edu.eg

Ahmed M. R. Fath El-Bab
Mechatronics and Robotics Engineering Dept.,
Egypt-Japan University of Science and Technology
Alexandria, Egypt
e-mail: ahmed_rashad@yahoo.com

Zakarya Zyada
Faculty of Mechanical Engineering FKM
University Teknologi Malaysia UTM
Johor, Malaysia
e-mail: zakarya@utm.my

Said M. Megahed
Mechanical Design and Production Engineering Dept.,
Cairo University
Giza, Egypt
e-mail: smegahed@ejust.edu.eg

Abstract— **Landmines are major problems, waste life and money. Much recent research acknowledges that the contact sensors have promising potential. In this work, a new idea of contact sensor for landmine detection is introduced. The sensor main principle is based on the concept of 2-DOF vibration absorber system (two springs and two masses), to detect the existence of an object (ex: landmine) in sand which is modeled as a 3rd spring. The sand stiffness (the 3rd spring stiffness k_o) can be acquired as function of the frequency vibration absorber mode ω_{Abs} (the frequency at which the 2nd mass has the lowest amplitude (mathematically proven: zero)). When the sand stiffness changed due to the presence of the landmine, the vibration absorber frequency ω_{Abs} changes, and consequently the landmine can be detected. The mathematical derivation of the (ω_{Abs}-k_o) relation is verified by simulations with Matlab and with finite element COMSOL Multi-physics. The system is succeeded to measure the sand stiffness up to 100kN/m. A physical prototype for the sensor is developed with sensitivity 16.85 (N/m)/Hz.**

Keywords- Contact sensing; finite element; Landmine detection; vibration; vibration absorber.

I. INTRODUCTION

The presence of landmines causes major problems in many regions in the world, because they restrict the development in such regions and also increase the personal risk. There are more than 100 countries affected by Landmines, UneXploded Ordnances (UXO), and Explosive Remnants of War (ERW). About, 20 countries are heavily-affected [1]. Sensing systems used for landmine detection are expensive and very critical in the demining process [2]. Many sensing technologies and studies are introduced. The most mature technologies are based on the electromagnetic waves (like Electromagnetic induction metal detector (MD), magnometers, and Ground penetration radar (GPR)) [3].

The Humanitarian Demining Standards for clearance success must satisfy 99.6% to 200 mm depth (according to United Nation Department of Human Affairs (UNDHA)) and 100% (according to International Mine Action Standards (IMAS)). To reach such high grades, until now, manual procedure is mandatory (that uses 'prodding' or 'probing' excavation tool) [4]. For this reason, Acoustic/Seismic and smart prodding are of the most promising technologies as they have Low false alarm, and properties feedback [5].

Many concepts have been introduced based on contact Acoustic/Seismic sensor. Martin et al. [6, 7, 8] studied the elastic-wave interactions with landmines and investigated 2-DOF model of surface-contacting vibrometer. Ground excitation is based on remote source while the moving vibrometer measures the associated ground surface motion, which is affected by the buried landmine when exists.

Donskoy et al. [9, 10, 11, 12] studied the nonlinear response of the 2-DOF model of the soil-mine system. The perturbation method used in the model introduces for the derived analytical solution to describe both quadratic and cubic acoustic interactions at the soil-mine interface. This solution has been compared with actual field measurements to obtain the nonlinear parameters of the buried mines, which have been analyzed with respect to mine types and burial depths. It was found that the cubic nonlinearity could be a significant contributor to the nonlinear response. This effect has led to develop a new intermodulation detection algorithm based on dual-frequency excitation.

Ishikawa et al. [13] modeled an active sensing prodder and mine as 2-DOF model. The prodder emits white Gaussian noise vibration to identify the object in front of the prodder by the frequency response and discrete Fourier transform.

Muggleton et al. [14] explored point vibration measurements to detect shallow-buried objects. The ground is modeled as single DOF at low frequency. A shaker is used to excite the ground vertically and has a built in impedance head which senses both the applied force and the measured acceleration. Resonance frequency and acceleration are used to detect buried pipes, but mechanical fatigue may occur.

Ali, et al. [15] studied the ground surface pressure distribution changes when applying static load. They studied objects (Anti-tank landmine, Anti-personnel landmine, rock, and can) exist under the ground at depths and inclination angles. That indicates a clear change in the ground surface

2166-0670/16 $31.00 © 2016 IEEE
DOI 10.1109/ISMS.2016.70

hardness and stiffness (around three times) especially at shallow objects.

In this study, based on the fact that the ground stiffness increases when a landmine exists, and the concept of 2-DOF vibration absorber, a novel stiffness sensor is modeled, simulated and fabricated. The measuring range of the sensor is selected to be associated with the sand-landmine problem. Then, a finite element model is developed to verify the sensor performance with the designed parameters. Sensitivity and linearity are calculated. Experiments are introduced with sensor prototype.

II. SENSOR MODEL

A. System Description

The sensor is modeled as 2-DOF system, where k_1, k_2, m_1, *and* m_2 are small spring stiffness, big spring stiffness, small mass, and big mass, respectively. While the ground stiffness is modeled as k_o (sensed object stiffness), as shown in Fig.1. The mass m_2 is affected with input sinusoidal force: $f_u = F_u \sin(\omega t)$, where F_u is the input force amplitude and ω is the input frequency, respectively. The system is designed to satisfy the vibration absorber phenomenon where:

$$\omega_{11} = \sqrt{k_1/m_1} = \omega_{22} = \sqrt{k_2/m_2} \quad \ldots\ldots\ldots\ldots\ldots\ldots\ldots\ldots (1)$$

At k_o equals zero (no object is in contact) and when the system operates at $\omega = \omega_{22} = \omega_{11}$ the vibration absorber phenomenon is accomplished (where the displacement of the mass m_2 equals zero and the whole the excitation energy is absorbed by the mass m_1. where the absorber part (m_1, k_1) exerts a force equals and opposites to the acting force on m_2 [16]. When the sensor contacts an object with certain stiffness k_o, the overall system natural frequencies are shifted and also the vibration absorber frequency ω_{Abs} of the phenomenon is also shifted. There is a direct relation between k_o and that frequency as will be proved next.

B. Mathematical Derivation

The free body diagram in Fig.1 shows the dynamic equations are as follow:

$$m_1\ddot{x_1} + (k_o + k_1)\,x_1 - k_1x_2 = 0 \quad \ldots\ldots\ldots\ldots\ldots\ldots\ldots\ldots (2)$$

$$m_2\ddot{x_2} + (k_1 + k_2)x_2 - k_1x_1 = f_u \quad \ldots\ldots\ldots\ldots\ldots\ldots\ldots\ldots (3)$$

By solving the differential eq's, the amplitudes X_1, X_2 are:

$$X_2 = \frac{\left[\frac{F_u}{k_2}\right]\left[\left(1+\frac{k_o}{k_1}\right) - \left(\frac{\omega}{\omega_{11}}\right)^2\right]}{\left[\left(1+\frac{k_1}{k_2}\right) - \left(\frac{\omega}{\omega_{22}}\right)^2\right]\left[\left(1+\frac{k_o}{k_1}\right) - \left(\frac{\omega}{\omega_{11}}\right)^2\right] - \frac{k_1}{k_2}} \quad (4)$$

$$X_1 = \frac{[F_u/k_2]}{\left[\left(1+\frac{k_1}{k_2}\right) - \left(\frac{\omega}{\omega_{22}}\right)^2\right]\left[(1+\frac{k_o}{k_1}) - \left(\frac{\omega}{\omega_{11}}\right)^2\right] - \frac{k_1}{k_2}} \quad \ldots (5)$$

A vibration absorber phenomenon occurs at: $X_2 = 0$

$$\left[(1+\frac{k_o}{k_1}) - \left(\frac{\omega}{\omega_{11}}\right)^2\right] = 0 \quad \ldots\ldots\ldots\ldots\ldots\ldots\ldots\ldots\ldots (6)$$

$$X_1 = \frac{-F_u}{k_1} \quad \ldots\ldots\ldots\ldots\ldots\ldots\ldots\ldots\ldots\ldots\ldots\ldots (7)$$

So that, the frequency causes the vibration absorber phenomenon:

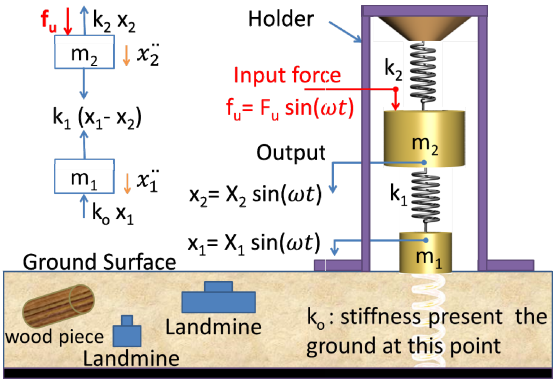

Fig.1. Sensor physical model and free body diagram.

$$\omega_{Abs} = \sqrt{\omega_{11}^2\left(1+\frac{k_o}{k_1}\right)} \quad \ldots\ldots\ldots\ldots\ldots\ldots\ldots\ldots\ldots\ldots (8)$$

Thus the ground stiffness k_o and the frequency (ω_{Abs}), at which the vibration absorber phenomenon occurs can be expressed as follows:

$$\boldsymbol{k_o = k_1\left(\frac{\omega_{Abs}^2}{\omega_{11}^2} - 1\right)} \quad \ldots\ldots\ldots\ldots\ldots\ldots\ldots\ldots\ldots\ldots (9)$$

III. MEASURING RANGE OF SAND-LANDMINE PROBLEM

Unlike Young's modulus, stiffness isn't only dependent on the material property of an object, but also on its dimensions. It is assumed that, the ground material is homogeneous elastic and incompressible. If the ground is excited by a vertical force, f_u, acting over an indentor of radius r as shown in Fig. 2, the local static stiffness of the land k_o can be expressed as follows [17]:

$$E = \frac{(1-\nu^2)F}{2rd} \quad \ldots\ldots\ldots\ldots\ldots\ldots\ldots\ldots\ldots\ldots\ldots\ldots (10)$$

$$k_o = \frac{F}{d} = \frac{2rE}{(1-\nu^2)} \quad \ldots\ldots\ldots\ldots\ldots\ldots\ldots\ldots\ldots\ldots\ldots\ldots (11)$$

Where: h, d, E, *and* ν are the ground height from rigid rock, indentation depth, the Young's Modulus, and Poisson's ratio of the ground respectively.

From Equation (11), to estimate the stiffness measuring range, it is required to choose the indentor radius, and the Young's Modulus range. From literature, the Young's modulus values of typical medium uniform sand: 30- 50

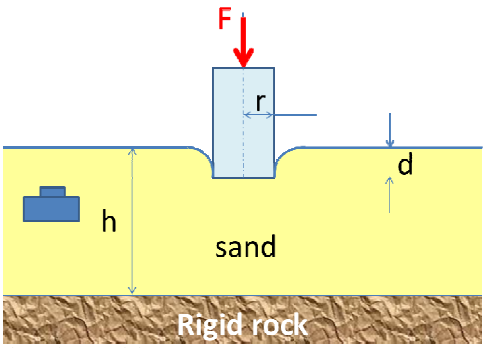

Fig.2. Indentation model parameters.

MPa [18, 19, 20, 21]. Base on the sand-landmine finite element model, the stiffness of the sand above landmine increases around three times [15]. In this model Young's Modulus range is selected be up to 150 MPa (50MPa x 3) to represent the presence of landmine with the indentor radius is 5 mm. By applying Equation (11), the stiffness measuring range can be estimated as 0-2 MN/m.

IV. Criterion of Parameters Selection Considering Vibration Absorber System

This section states the criterion for selecting the sensor parameters (m_1, k_1, m_2, *and* k_2) as follows:

1) First of all, the (springs stiffness / the masses) ratio must satisfy the vibration absorber Equation (1).
2) To get clear phenomenon occurrence (easily find zero displacement at m_2), $m_1/m_2 = 0.5$ is considered [16].
3) The relation between ω_{Abs}-k_o derived in Equations (8, 9), should be linear through the working range, in order to keep constant sensitivity along the measuring range.
4) The sensitivity value ($d\omega_{Abs}/dk_o$), which is adapted by (k_1, and m_1) should be as large as possible to reach high accuracy when obtaining the object stiffness k_o.
5) The masses m_1 and m_2 should be as small as possible in order to not activate the landmine.
6) The masses m_1 and m_2 should be as small as possible in order increase the frequency range at certain k_1, and k_2.

V. Mathematical Modeling and Simulation

A. Mathematical Model

In this section, the frequency responses of x_1 and x_2, the displacements of the lumped masses m_1 and m_2, respectively, are determined, based on Equations (4, 5) using MATLAB. After that, the frequency at which the vibration absorber phenomenon occurs (zero displacement at m_2) is determined using the flowchart shown in Fig.3. The relation between the sand stiffness (k_o) and the corresponding frequency (ω_{Abs}), at which the vibration absorber occurs is determined as for the selected design parameters: m_1= 0.0017 kg, k_1= $1.78\text{x}10^3$ N/m (based on the available Piezo actuator in Fig.4), m_2= 2 m_1, and k_2= 2k_1 (criteria 1 and 2 are applied here). The normalized displacements, of the two masses vs. the excitation frequency, are presented in Fig.5, at certain k_o.

From the Fig.5.a, and at k_o= 0 N/m (blue curve), it is shown that the vibration absorber phenomenon is happened at frequency $\omega = \omega_{Abs}$= 161.2 Hz, where the x_2 response equals zero. For the same sensor parameters but at different ground stiffness values: k_o= [10^4, 10^5] N/m, the corresponding vibration absorber frequencies are different. As presented in Fig.5.b, it is clear that this relation is nonlinear. For this reason the sensor parameters should be properly selected to fulfill the criteria in section 4. In the next section a finite element method will be utilized to determine the vibration absorber frequency of the sensor system when subjected to different land stiffness k_o. The sensor dimension will be selected to fulfill the selection criteria 3, 4, 5, and 6 in section 4.

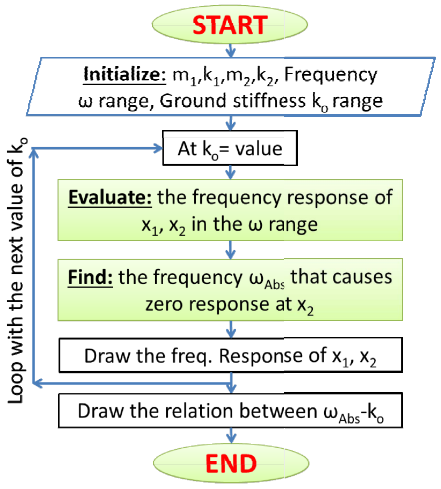

Fig.3. Flow chart of the mathematical model algorithm.

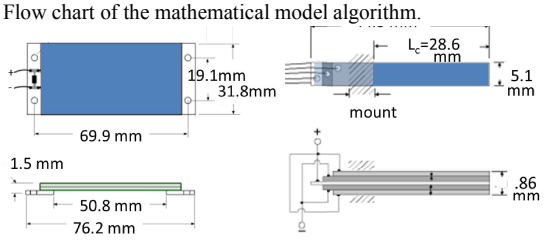

Fig.4. PIEZO SYSTEMS: D220-A4-503YB and T434-A4-201

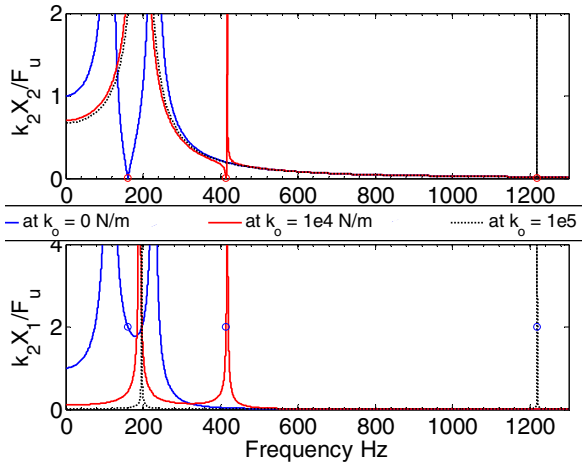

(a) x_2, x_1 frequency response

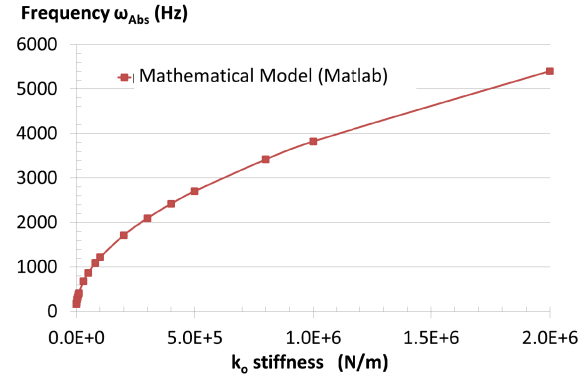

(b) Direct relation between ω_{Abs}-k_o

Fig.5. Frequency response at certain ground stiffness k_o values, and the corresponding vibration absorber frequency ω_{Abs}.

B. Finite Element model (with COMSOL Multiphysics)

In this section the sensor parameters (m_1, k_1, m_2, and k_2) and its dimension will be selected to verify the resultant sensitivity and linearity of the sensor. The sensor parameters will take values based on the commercial Piezo-electric actuators cantilever system as shown in Fig.6. The two springs k_1 and k_2, which are shown in Fig.1 are presented by the stiffness of the cantilever beams. The masses m_1 and m_2 which in Fig.1 is represented by the equivalent masses of the two Piezo-electric cantilever plus the concentrated masses which shown in Fig.6.

The Piezo-electric actuators are chosen here because they produce excitation with high frequency range more than the frequency range offered by commercial motors which used in the excitation systems such as rotating mass unbalance or cam-follower.

The COMSOL model: Type: 2D Solid Mechanics

Material: Piezo-ceramic, Lead Zirconate Titanate, Piezo Systems Material Designation Type 5A4E (Navy Type II)

Elastic Modulus: 52GPa, Poisson's: 0.38, Density: 8216Kg/m^3

Geometry: As shown in Fig.7, two block for the two masses and two beams for the two springs.

Beam1 width= Beam2 width=28.6 mm,

Mass1= 1.5 gm, Mass2= 3 gm.

Note: the mass m_1 in the mathematical modeling and MATLAB simulation is the equivalent mass [16]:

$$m_1 = Mass1 + \frac{beam1\ mass}{4} \quad \ldots\ldots\ldots\ldots\ldots\ldots\ldots\ldots\ldots\ldots (12)$$

Beam thickness (t) = 0.86mm, Where the stiffness relation:

$$k = \frac{Ewt^3}{L_c^3} \quad \ldots\ldots\ldots\ldots\ldots\ldots\ldots\ldots\ldots\ldots\ldots\ldots\ldots\ldots\ldots (13)$$

Where: E, w, t, and L_c are the Young's Modulus, width, height, and length.

Solid Mechanics:

Boundary conditions: fixed from left.

Boundary load: applied at the end of the beam2, harmonic perturbation force per unit length in y direction: 5x10^2 N/m.

Spring foundation to represent the object stiffness (the ground in our case), at each beam thickness we will find the sensor output frequency with different land stiffness: k_o= [0-2x10^6] N/m.

Meshing: the system is meshed by:

Type: free Triangular. Size: extremely fine.

VI. Simulation Results

In this section the two natural frequencies, the mode shapes, and the vibration absorber frequency of the system (which composed of Piezo Systems: T434-A4-201), are determined.

The effect of changing the sand stiffness (k_o) on the sensor vibration absorber frequency is shown in Fig.8, the simulation results is presented for (k_1 =1.78 kN/m). The sensitivity is (9.85 Hz/(KN/m)) in the range (0-100 kN/m). The linearity is (R^2=0.96) in the range (0-100 kN/m), while

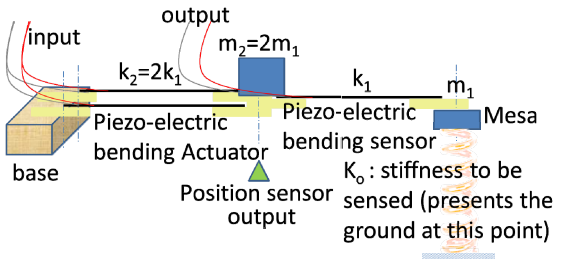

Fig.6. Piezo-electric version of the proposed sensor

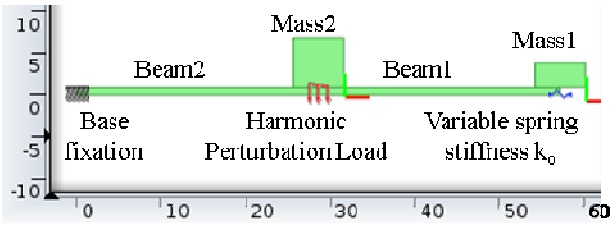

Fig.7. Finite element COMSOL model 2D beam model, load and boundary constrains

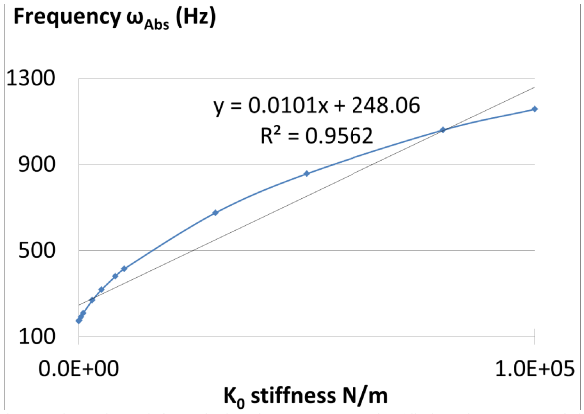

Fig.8. Linearity of the relation between ω_{Abs}-k_o (finite element model) k_o range (0 – 2 MN/m) at (k_1=1.78 kN/m).

for the range (0-2MN/m), the linearity is decreased to (R^2=0.37).

Figure 8 shows that, this design dimension couldn't satisfy the required measurement range 0- 2 MN/m because saturation occurs after stiffness (k_o) = 2x10^5 N/m. Also another problem appears that the vibration absorber frequency (ω_{Abs}) is very close to the upper natural frequency of the system in the range up to k_o = 10^5 N/m, as shown in

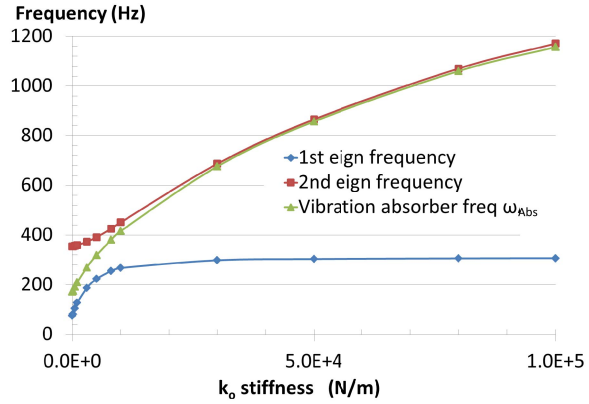

Fig.9. Sensor frequencies when changing stiffness k_o at (k_1=1.78 kN/m).

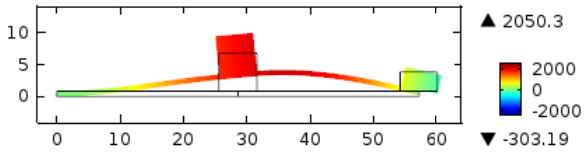

(a) Y-displacement (mm), 1st natural frequency at 306.6 Hz

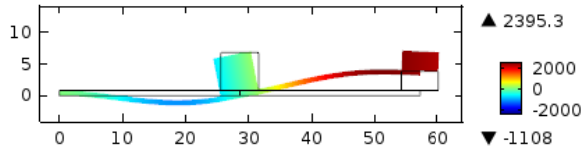

(b) Y-displacement (mm), 2nd natural frequency at 1170.80 Hz

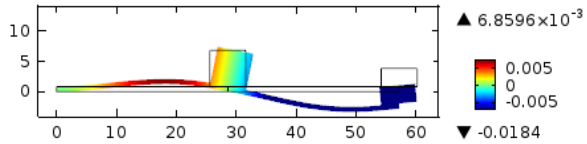

(c) Y-displacement (mm), Vibration absorber phenomenon at frequency ω_{Abs}=1156.83 Hz when displacement =0 at m_2.

Fig.10. finite element COMSOL model responses at ground stiffness k_o = 10^5 N/m and (k_1=1.78 kN/m).

Fig. 9. This means it is difficult to distinguish the vibration absorber frequency (ω_{Abs}), during changing the excitation frequency. At k_o= 10^5 N/m the difference between the second natural frequency and the vibration absorber frequency is very small around 14 Hz, which is one of the drawbacks of this design parameter value (k_1=1.78 kN/m).

The natural frequencies modes and the vibration absorber mode of the sensor are shown in Fig.10. It is clearly shown that the 1st and 2nd natural frequencies have maximum displacement of 2050 and 2395 mm respectively; while at the vibration absorber mode, it is only 7µm. From This point, the presented novel sensor has advantages, because it works at the vibration absorber mode where low displacement occurs.

VII. EXPERIMENTAL WORK

In this section a prototype is produced to validate experimentally that the contact sensor (2-DOF vibration absorber based) can be used in stiffness measurements. The experimental setup is prepared, then the sensor behavior is investigated at no contact and at contact with five different objects stiffness k_o.

As shown in fig.4 and fig.11, the sensor prototype consists of two cantilevers which are produced to satisfy the criterion on section 4, using the PIEZO SYSTEMS: D220-A4-503YB bending actuators. Where the system parameters are: k_1=188 N/m, m_1= 3.4+10.3/4 =6 gm, k_2=2k_1, m_2= 2m_1

As shown in fig. 12, the experimental setup consists of the sensor prototype, signal generator, amplifier, position sensor, oscilloscope and Acrylic (PMMA) cantilevers (represent the stiffness objects to be measured)

The sensor response is investigated at no contact (k_o =0) and at contact with stiffness as shown in Table I. We must note that the noise in the system is recorded to be 90 mv, which leads to that the actual amplitude of the vibration absorber mode is nearly zero, as proven mathematical in section 2. Figure 13 shows that the relation between the stiffness k_o and the 3 modes can be divided into three zones of each: linear zone, nonlinear zone, and saturation zone.

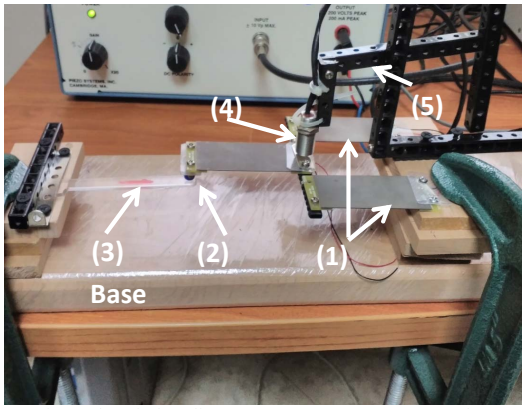

(1) Two Piezo-electric bending Actuators (2) Indentor
(3) Test specimen 1 with stiffness k_o (4) Position sensor probe
(5) Position sensor level adjustment mechanism

Fig.11. sensor prototype

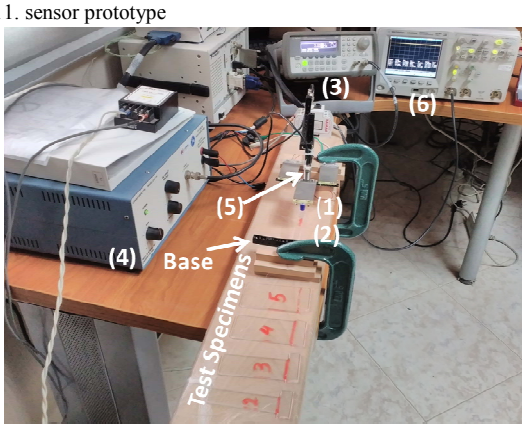

(1) The sensor Prototype (2) Test specimen 1 (3) Function generator
(4) Linear Amplifier (5) position sensor probe (6) Oscilloscope

Fig.12. Experimental setup

TABLE I
FREQUENCY MODES AT DIFFERENT SPECIMENS STIFFNESS

Stiff.	1st resonance mode		Vib. Abs. mode		2nd resonance mode	
k_o (N/m)	Freq. (Hz)	pk-pk (v)	Freq. (Hz)	pk-pk (v)	Freq. (Hz)	pk-pk (v)
0	13	8.4	28	0.08	56	2.3
278	28	2	45	0.13	60	1.4
556	33	1.1	61	0.08	63	0.8
834	36	1.1	65	0.09	67	0.5
1112	38	1.1	69	0.09	71	0.4
1390	39	1.1	70	0.09	71	0.4

It is clear that: The 1st resonance frequency-stiffness (ω_1-k_o) relation is the most critical (high pk-pk) and lower sensitivity and linearity. The 2nd resonance frequency-stiffness (ω_2-k_o) relation has wider linearity range than the others. The vibration absorber frequency-stiffness (ω_{Abs}-k_o) relation has the highest sensitivity in the linear zone. Sensitivity= 16.85 (N/m) / Hz.

VIII. CONCLUSION

New model of contact stiffness sensor has been introduced with a design procedure for landmine detection,

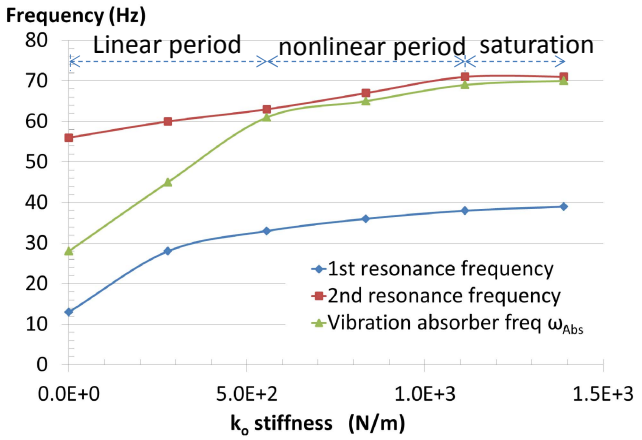

Fig.13. Experimental work, frequencies change when changing stiffness k_o Range (0-1500 N/m) at (k_1 =188 N/m)

based on the concept of 2-DOF vibration absorber system. It consists of 2 springs and 2 masses, to detect a third spring (landmine presence in sand). The 3rd spring stiffness can be measured as function of the vibration absorber frequency (ω_{Abs}). The changes in sand stiffness due to landmine, causes changes in the vibration absorber frequency ω_{Abs}, and subsequently the landmine can be detected.

The main advantage of this idea is that the frequency (ω_{Abs}) searching is done away from the resonance points of the system.

The measuring range of the sensor is chosen to be associated with typical sand Young's modulus values: up to 150 MPa and at indentor radius 5 mm. This gives the stiffness range (0-2 MN/m).

Simplified mathematical model has been introduced and simulated with MATLAB and verified with finite element with COMSOL.

The sensor design parameters are selected to satisfy the vibration absorber phenomenon. The design parameter values are verified to be k_1=1.78 kN/m, k_2= 3.56 kN/m, m_1=2.5 gm, m_2 = 5 gm. Finite element model proved that the propose sensor can detect different sand stiffness in the range 0-100 kN/m. It give as high sensitivity as 9.85 Hz / (kN/m) and linearity (R^2= 96%), but lower linearity in the stiffness range (0-2 MN/m).

Experimental prototype is developed to prove the concept which indicates that the vibration absorber frequency-stiffness (ω_{Abs}-k_o) relation has the highest sensitivity in the linear zone. Sensitivity= 16.85 Hz / (N/m)

ACKNOWLEDGMENT

This research is funded by the Egypt-Japan University of Science and Technology (EJUST), Alexandria, Egypt.

REFERENCES

[1] Said M. Megahed, Hussein F.M. Ali, and Ahmed H. Hussein: "Egypt Landmine Problem: History, Facts, Difficulties and Clearance Efforts", International Symp. Humanitarian Demining, Šibenik, Croatia, (2010).

[2] Furuta, Katsuhisa; Ishikawa, Jun (Eds.): "Anti-personnel landmine detection for humanitarian demining", springer (2009).

[3] "Detectors and Personal Protective Equipment Catalogue 2009", GICHD: Geneva Int. Centre for Humanitarian Demining, (2009).

[4] M.Habib: "Humanitarian Demining Innovative Solutions and the Challenges of Technology",ARS Publisher, (2008).

[5] Macdonald, J., Lockwood, J.R., Mcfee, J., Altshuler, T., Broach, T., Carin, L., Harmon, R., Rappaport, C., Scott, W. and Weaber, R.: "Alternatives for Landmine Detection" (Pittsburg, PA: RAND), (2003).

[6] Waymond R. Scott Jr., James S. Martin, and Gregg D. Larson: "Experimental Model for a Seismic Landmine Detection System", IEEE Transactions on Geoscience and Remote Sensing, vol. 39, no. 6,(2001).

[7] James S. Martin, Gregg D. Larson, and Waymond R. Scott Jr.: "Surface-Contacting Vibrometers for Seismic Landmine Detection", Proc. of SPIE Vol. 5794, Bellingham, WA,(2005).

[8] James S. Martin, Gregg D. Larson, and Waymond R. Scott Jr.: "An investigation of surface-contacting sensors for the seismic detection of buried landmines", J. Acoust. Soc. Am., Vol. 120, No. 5, (2006).

[9] D. M. Donskoy,A. Reznik, A. Zagrai, and A. Ekimov: "Nonlinear vibrations of buried landmines", J. Acoust. Soc. Am. 117 (2), (2005).

[10] D. M. Donskoy: "Nonlinear vibro-acoustic technique for land mine detection", SPIE's Proceedings on Detection and Remediation Technologies for Mines and Minelike Targets III, Vol. 3392, (1998).

[11] D. Donskoy, A. Ekimov, N. Sedunov, and M. Tsionskiy: "Nonlinear seismo-acoustic land mine detection and discrimination", J. Acoust. Soc. Am. 111(6), 2705-2714, (2002).

[12] D. Donskoy, A. Ekimov, N. Sedunov, and M. Tsionskiy: "Nonlinear seismo-acoustic land mine detection: Field test", SPIE's Proceedings on Detection and Remediation Technologies for Mines and Minelike Targets VII, Vol. 4742, pp. 685-695, (2002).

[13] Jun Ishikawa, and Atsushi Iino: "A Study on Prodding Detection of Antipersonnel Landmine Using Active Sensing Prodder", International Symposium: Humanitarian Demining 2010, Šibenik, Croatia, (2010).

[14] J.M. Muggleton, M.J. Brennan, and C.D.F. Rogers: "Point vibration measurements for the detection of shallow-buried objects", Tunnelling and Underground Space Technology (39) 27–33, (2014).

[15] Hussein F.M. Ali, Zakarya Zyada, Ahmed M. R. Fath El Bab, and Said M. Megahed: "Inclination Angle Effect on Landmine Characteristics Estimation in Sandy Desert using Neural Networks", The 10th Asian Control Conference (ASCC 2015), (2015).

[16] W. T.Thomson:"Theory of Vibration with Applications", Springer US,1993.

[17] J. W. Harding, I. N. Sneddon: "The elastic stresses produced by the indentation of the plane surface of a semi-infinite elastic solid by a rigid punch", Mathematical Proceedings of the Cambridge Philosophical Society, Volume 41, Issue 01, pp.16-26, (1945)

[18] Obrzud R. and Truty A.: "The Hardening Soil Model - A Practical Guidebook", Z Soil. PC 100701 report, revised 31.01.2012

[19] Kezdi, A. "Handbook of Soil Mechanics". Elsevier, Amsterdam, (1974).

[20] Prat, M., Bisch, E., Millard, A., Mestat, P., and Cabot, G. "La modelisation des ouvrages". Hermes, Paris, (1995).

[21] Geotechdata.info, "Soil Young's modulus", site: http://geotechdata.info /parameter/soil-elastic-young-modulus.html (09.2013), check 09-2015.